

Investigation of Geometric Characteristics on the Lubricant Performance of Thrust Bearing with Cavitation

L. Kailei¹, C. Jiayuan¹, Z. Haoran¹, Z. Lin¹, W. Xuze² and C. Yu^{1†}

¹ School of Mechanical Engineering, Jiangsu University of Technology, Changzhou, Jiangsu 213016, China

² School of Information and Intelligent Engineering, Zhejiang Wanli University, Ningbo, Zhejiang 315100, China

†Corresponding author: chenyu@jsut.edu.cn

ABSTRACT

In this study, a mixed lubrication model that incorporates cavitation can be developed to examine the evolution of hydrodynamic lubrication in spiral grooved thrust bearing. The simulation model includes cavitation effects and utilizes hexahedron unit grid division technology to enhance the mesh quality of spiral grooved thrust bearing. The computational model would be crafted to provide an efficient solution while maintaining the ability to accurately represent the hydrodynamic behavior of spiral grooved thrust bearing. The simulation model considers the impact of geometric characteristics and operational conditions, including the viscoelastic effect, transformation feature, and flow state, to enhance calculation ability. The validity and practicality of the proposed approach are corroborated by experimental results. Additionally, an analysis of the hydrodynamic behavior of spiral grooved thrust bearing can be conducted, and the simulation results elucidate the relationship between key parameters and lubrication performance, offering valuable insights for the optimization of spiral grooved thrust bearing.

Article History

Received October 16, 2024

Revised December 25, 2024

Accepted February 10, 2025

Available online May 5, 2025

Keywords:

Thrust bearing

Geometric characteristics

Groove effect

Lubrication performance

1. INTRODUCTION

Typically, the oil film of spiral grooved thrust bearing (SGTB) is assumed to be imbued with a lubrication medium in hydrodynamic behavior analyses. However, the presence of specific physical characteristics and structural parameters can induce variations in the hydrodynamic response, such as changes in viscosity, density, and spiral geometry. These factors are pivotal in analyzing the lubrication performance of SGTB under conditions of cavitation, potentially representing a significant area of application. A fundamental challenge is delineating the relationship between the pressure characteristics of the lubricant film and the physical properties of the lubricant mediums under cavitation conditions. Such analyses must consider the phase transformation characteristics and model parameters. Additionally, essential lubricant parameters like density, viscosity, and thermal conductivity are determined through experimental analysis. Another critical issue is assessing how the grooved geometric characteristics influence the distribution of cavitation, which in turn impacts the accuracy of hydrodynamic response assessments for SGTB. It can be evident that these geometric characteristics significantly alter the ability of SGTB. Thus, it is essential to identify a suitable

simulation model that accurately represents the hydrodynamic response of SGTB and mitigates adverse effects.

The computational and analytical approaches of thrust bearing are the main points of study, which mainly includes the methods of establishing the simulation model and lubrication performance analysis of structural parameters (Meng et al., 2014; Rao et al., 2019;). Eleshaky (2009) developed the simulation model of thrust bearing by CFD method, which discussed the effects of element type on the accuracy of simulation and revealed the variation of lubrication characteristics. With the groove shapes taken into account, Fesanghary and Khonsari (2013) designed the hydrodynamic experiment platform of parallel flat surface bearing and the results plotted the pressure distribution characteristics, which guided the direction of bearing design with spiral grooves. Moreover, Zhang et al. (2013) described the nonlinear dynamic behavior of bearing by a new approach and the influences of temperature on the dynamic response of thrust bearing. Ochiai et al. (2014) performed an effective model to describe the angular displacement characteristics of thrust bearing. Based on the method of computational fluid dynamics, the mapping characteristics of geometric parameter and

lubricant performance was investigated. The conservation equation of mass and momentum was resolved by Gao et al. (2015), and the reason of lubrication performance changed by input pressure was the main points of discussion. For purpose of obtained a better hydrodynamic lubrication of thrust bearing with spiral grooved, Xu and Yang (2016) conducted the investigation of modelling and analysis detailedly. The increase of oil-film pressure was the key factor of hydrodynamic ability, and a bigger supporting stiffness was also obtained. Moreover, Gropper et al. (2018) expanded the calculation approach for solving N-S equation and continuity, which conducted the iteration by least square method. Compared with tradition methodology, the proposed approach not only ensured calculation accuracy, but also reduced the computational time. Pavel et al. (2019) introduced the fast-solution method into the hydrodynamic analysis model of bearing, and it was also employed to describe the hydrodynamic behavior of similar productions. The effects of inlet temperature, input pressure and bearing lubricant layer were obtained.

The cavitation effects always appear in the lubrication medium of bearing (Meng et al., 2015; Kim et al., 2020). Wu et al. (2015) developed an approach for describing the pattern characteristics of thrust bearing in the variable operation condition. The multiple phases feature of lubricant medium could be discovered and the reason of transmission phase would be illustrated by the numerical result. The influence of micro-structure feature on the bearing capacity was studied by Mao et al. (2016). The geometrical parameter and structure features played important roles on the flow characteristics of oil-film, especially in the near solid region. It was a noteworthy content of design and analysis for bearing. Gherca et al. (2019) presented computation method of lubrication performance for thrust bearing by finite difference method. The introduce of node and element could refine the simulation model and the distribution feature may be revealed in different flow states. Meanwhile, the pressure distribution of oil-film was changed by the flow state. In order to improve the calculation accuracy, Hu & Meng (2019) proposed a new analysis method for illustrating the hydrodynamic behavior of SGTB. The numerical result was compared with test results, and the variation trends explained the effectiveness of presented method. Furthermore, the transmission phase of oil and air was always attracted in the study of thrust bearing. Based on the rupture boundary condition, Lin et al. (2020) established the hydrodynamics equations of thrust bearing, which included the relationship between minimum thickness and rupture pressure value of oil-film. The results showed that the cavitation effects would be illustrated clearly by proposed method.

In the present study, the primary content is to develop an effective approach for predicting the lubrication behavior of SGTB. The research primarily explores the relationship between structural parameters and lubrication performance in the presence of cavitation under various operational conditions. It incorporates phase transition characteristics and cavitation regeneration conditions into the tribological analysis of

SGTB, utilizing a simulation model based on hydrodynamic theory. To enhance the efficiency of solutions, the cavitation effect is represented using a multiphase model, and various lubricated mediums are considered within the lubricant film. Additionally, this study examines how structural parameters and operational conditions influence the lubrication characteristics of SGTB, focusing also on variations in pressure and energy loss.

2. MATHEMATICAL MODEL

The geometric characteristics of SGTB are illustrated in Fig. 1. It is apparent that the groove plays a crucial role within the SGTB, and the surface depth of the SGTB varies between different areas (land and groove) (Bai & Bai, 2014; Zouzoulas & Papadopoulos 2017). The groove's shape resembles a spiral line within the global coordinate system, which is characterized by the spiral angle (α) and the base radius of the spiral curve (r_b). In the model, the inner radius of the spiral groove is defined as r_{in} , while the outer radius is denoted as r_{out} . The mathematical representation of the spiral groove is provided as follows:

$$r = r_b e^{\theta \tan \alpha} \quad (1)$$

Lubrication oil is filled with clearance (h) of thrust bearing, which includes the thickness of land (h_l) and groove (h_g). The equation is given as:

$$h = h_l \quad (2a)$$

$$h = h_l + h_g \quad (2b)$$

During motion, the molecules of the lubrication medium must adhere to the equations of mass conservation and momentum conservation (Lin et al., 2018; Zhang et al., 2018). These equations incorporate the fluid density (ρ_f), the fluid velocity vector (\vec{v}), and viscosity (μ), which determine the motion characteristics. Consequently, the relationship concerning fluid mass can be summarized by the following equations:

$$\frac{\partial \rho_f}{\partial t} + \nabla \cdot (\rho_f \vec{v}) = 0 \quad (3)$$

The momentum includes static pressure (P), gravity of molecule (\vec{g}) and external load (\vec{F}), and the equation is written as:

$$\frac{\partial}{\partial t} (\rho \vec{v}) + \nabla (\rho \vec{v} \vec{v}) = -\nabla P + \nabla(\vec{\tau}) + \rho \vec{g} + \vec{F} \quad (4)$$

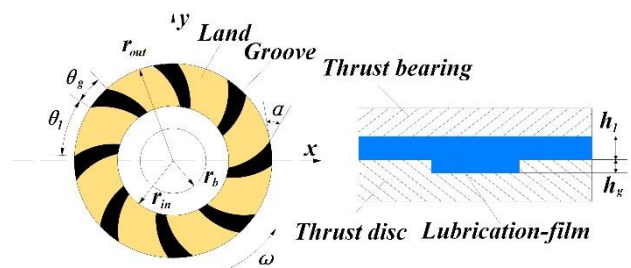


Fig. 1 Geometrical configuration of SGTB

where $\bar{\tau}$ denotes stress tensor and it is described as:

$$\bar{\tau} = \mu \left[(\nabla \vec{v} + \nabla \vec{v}^T) - \frac{2}{3} \nabla \cdot \vec{v} I \right] \quad (5)$$

where I represents the unit tensor.

Owing to the occurrence of cavitation, it is necessary to address the transition and components of the phase. Mixture density (ρ_m) is pivotal in describing the hydrodynamic behavior of the lubrication medium, which is changed by vapor mass fraction (f) (Chetti 2016; Zhao et al., 2016). Furthermore, the characteristics of cavitation are influenced by the velocity of the vapor phase (\vec{v}_v) and the effective exchange coefficient (γ). The mass transfer between liquid and vapor phases (generation and rupture) is described by:

$$\frac{\partial}{\partial t} (\rho_m f) + \nabla (\rho_m \vec{v}_v f) = -\nabla (\gamma \nabla f) + R_e - R_c \quad (6)$$

in which R_e denotes vapor generation and R_c is condensation rate.

As the evaluated characteristics of SGTB, a higher supporting capacity and lower energy loss are looked forward, which is related with pressure (p) and shear force (τ) of lubrication-film. Based on oil-film pressure, the bearing capacity can be written as:

$$W = \int_0^{2\pi} \int_{R_{in}}^{R_{out}} p r dr d\theta \quad (7)$$

The friction and friction coefficient also are given as below:

$$F = - \int_0^{2\pi} \int_{R_{in}}^{R_{out}} \tau r dr d\theta \quad (8)$$

$$f = F/W \quad (9)$$

The bearing stiffness (K) and damping coefficient (D) are the important role for evaluating the performance of SGTB, which can be obtained by load carrying capacity (W) and rotation speed (ω). The expression is given by:

$$K = \frac{W(h_g - \Delta h_g) - W(h_g)}{\Delta h_g} \quad (10)$$

$$D = \frac{K}{\omega} \quad (11)$$

where Δh_g is slight variation of bearing gap.

3. COMPARISON AND ANALYSIS

3.1 Comparative Analysis

The accuracy and effectiveness of simulations are crucial for evaluating the proposed model of the thrust bearing. Parameters of the thrust bearing (Hu & Meng 2019) are selected for a comparative analysis between simulation and experimental results. The rotational speeds of the thrust bearing ranged from 20 rpm to 1000 rpm, with the results depicted in Fig. 2. A noticeable difference between the experimental and simulation results was observed, with the maximum deviation occurring at 200 rpm. Below this speed, the friction

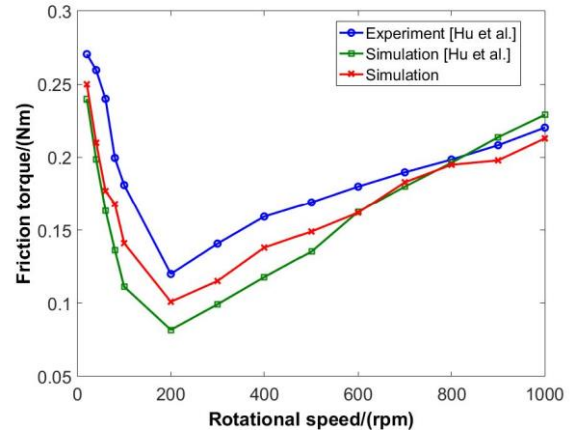


Fig. 2 Comparative analysis of thrust bearing

torque of the thrust bearing decreases. Above 200 rpm, the flow characteristics of the lubricant medium improve, enhancing intermolecular collisions. It is evident that the deviation between the simulation results using the proposed method and the experimental data is smaller than that of the original simulation model, with a mere difference of 0.019 Nm. Furthermore, the trend in simulation results closely aligns with the experimental data across various operating conditions. The proposed method in this study provides more accurate results, reducing the deviation between experiment and simulation. The results also demonstrate that the presented approach accurately represents the hydrodynamic behavior of SGTB.

3.2 Lubricated Medium Characteristics Analysis

Based on the hydrodynamic equations of SGTB, it is clear that the physical properties of the lubrication medium determine the pressure values, support characteristics, and friction torque. The structural characteristics and calculation parameter of SGTB are listed in Table 1. Additionally, the boundary conditions for the solution are defined. Initially, element division is a critical step in the simulation, and the quality of elements affects both the efficiency and accuracy of calculations. Considering the phase transition and sliding feature, the hydrodynamic model of SGTB is divided using hexahedral units with the oil film defined in 10 layers, as shown in Fig. 3. The mesh quality can be assessed by grade. All elements of mesh are lower than 0.6 ("0" is best), which can ensure higher accuracy and better efficiency. Moreover, the vaporization pressure is set at 2000 Pa, and the multiphase flow equation is solved using the SIMPLE algorithm. The maximum allowable iteration error is set at 10⁻⁵, and the mass flow rates at the inlet and outlet must be considered in the simulation. Further, relative references (Meng & Yang 2013; Zhang et al., 2018) indicate that turbulent flow often occurs in thrust bearings with lubricant oil due to higher Reynolds numbers and velocities. Thus, turbulent flow is incorporated into the simulation model in this work.

Oil and water are employed to explain the rheological characteristics has a significant influence on

Table 1 Structural characteristics and parameters

Parameters	Value
Inner radius r_{in} (mm)	17.4
Outer radius r_{out} (mm)	30
Based radius r_b (mm)	12
Inner radius r_{in} (mm)	17.4
Outer radius r_{out} (mm)	30
Lubricant density ρ (kg/m ³)	890
Lubricant viscosity ν at 20°C (Pa·s)	0.029
Lubricant thermal conductivity (W/(m·k))	0.13
Lubricant specific heat (J/(kg·k))	2000
Groove depth h_g (mm)	0.03
Land depth h_l (mm)	0.01

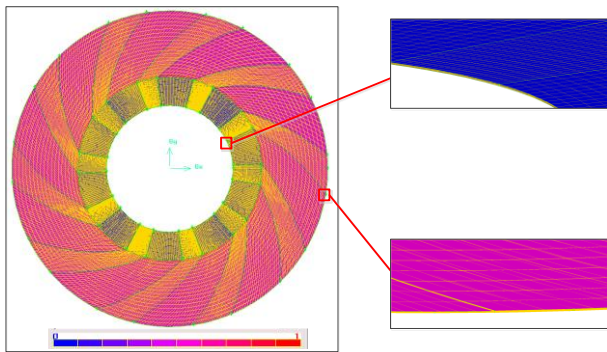


Fig. 3 Mesh divided model

the lubricant performance of SGTB. The structural characteristics is defined the same values ($\alpha=30^\circ$, $n=10$, $\omega=1500$ rpm and $w_t=0.58$).

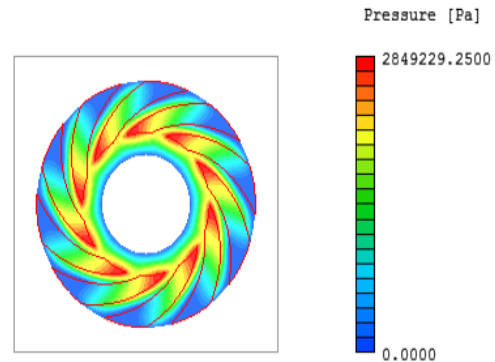
Figure 4 shows the influence of Newtonian fluid (water) and non-Newtonian fluid (oil) on hydrodynamic response of SGTB. The distribution pattern reveal that although the pressure characteristics of the lubrication film maintain a similar distribution, the actual pressure values differ significantly between oil (2.849 MPa) and water (0.196 MPa). Despite the increased molecular friction in the lubrication film, the bearing capacity of the SGTB using oil as a lubricant is higher. In contrast, the supporting characteristics of SGTB with water are lower. Due to changes in viscosity for different lubrication mediums, the shear force in an oil-lubricated system is affected by the shear rate. Additionally, the results suggest that the non-Newtonian fluid (oil) cannot exhibit optimal ability at high-speed rotational speeds.

4. RESULTS AND DISCUSSIONS

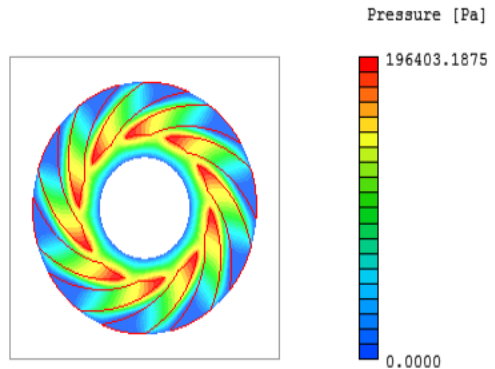
This section examines the coupled influence of structure characteristics and working conditions on lubricant performance of SGTB, focusing particularly on lubrication characteristics. The results elucidate the regular pattern of lubricant ability for SGTB in variable conditions.

4.1 Effects of Spiral Angle

As the main parameters, the characteristics of spiral angle is related with flow characteristics of oil-film



(a) Lubricated medium of oil



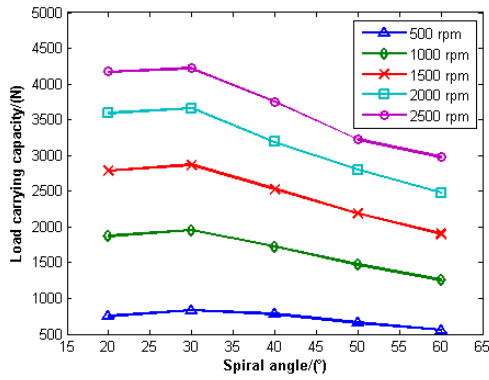
(b) Lubricated medium of water

Fig. 4 Pressure characteristics of SGTB

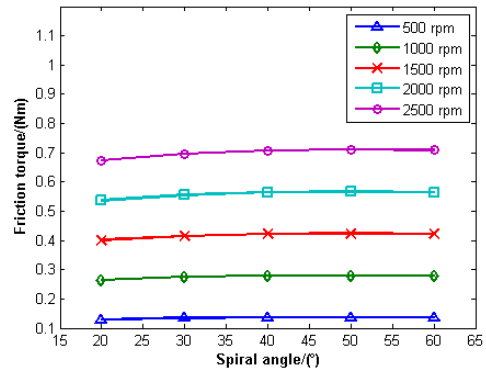
closely and it should be concerned in the structure design. The groove number and groove width ratio can be chosen as constants (10 and 0.58). Then, the rotational speeds and spiral angle are also selected with different values.

Figure 5(a) presents the influence of spiral angle on bearing capacity under various conditions. The data show that the load carrying capacity reflects changes in oil-film pressure. It is well-known that increasing the rotational speed enhances the flow characteristics of the lubrication medium, which, in turn, affects the oil-film and subsequently the bearing capacity. Notably, with a smaller spiral angle taken into, the load carrying capacity decreases, particularly at higher rotational speeds. The thickness of the oil-film, closely associated with the squeeze force exerted by molecules, also plays a critical role. An increase in oil-film thickness allows for greater motion space for fluid molecules, reducing the oil-film pressure. The spiral angle of the groove alters the oil-film thickness in different regions, impacting the bearing capacity of SGTB. Furthermore, Fig. 5(b) explores the relationship between working conditions and friction torque. The results indicate that the influence of the spiral angle on friction torque is minimal. Beyond a spiral angle of 30° , the friction torque remains relatively constant. The simulation also highlights how the spiral angle, rotational speed, and friction torque interrelate. The shear force exerted by fluid molecules is a determinant of friction torque, a critical design consideration for SGTB. Friction loss represents the energy loss between the SGTB and the oil-film.

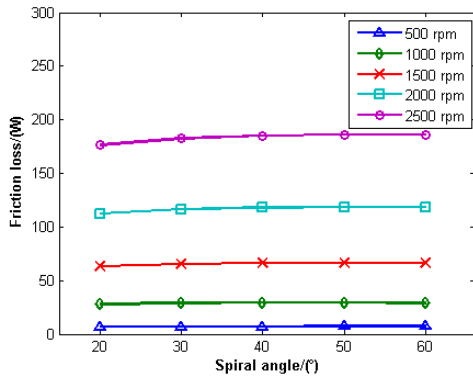
Figure 5(c) displays the friction loss for the thrust



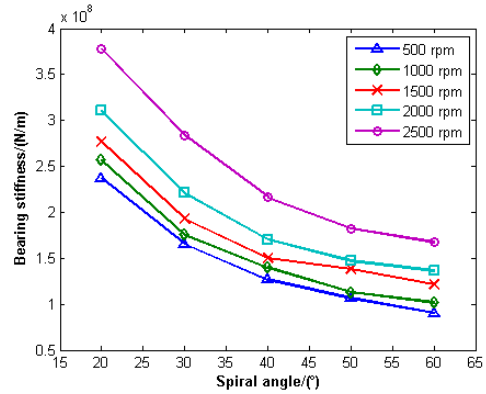
(a) Load carrying capacity



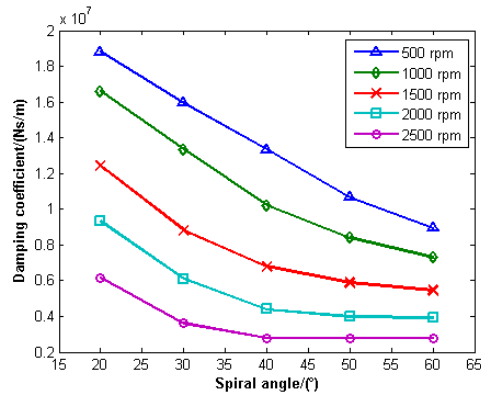
(b) Friction torque



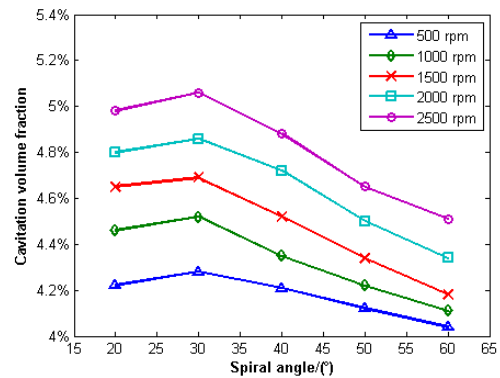
(c) Friction loss



(d) Bearing stiffness



(e) Damping coefficient



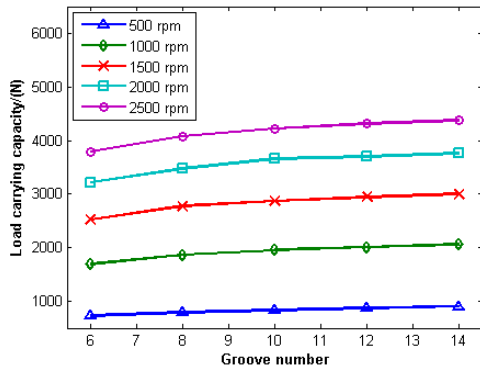
(f) Cavitation volume fraction

Fig. 5 Hydrodynamic behavior of SGTB with different spiral angles

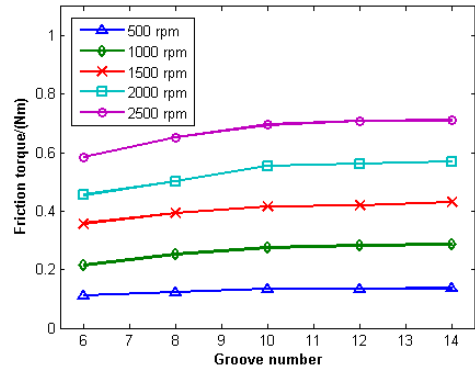
bearing under various conditions. Since friction loss is influenced by multiple factors, simulations are conducted considering both the spiral angle and rotational speed. The results show that the variation in friction loss is minimal when the rotational speed exceeds 2000 rpm, and this value remains fairly constant at lower speeds. The results also indicate that an increase in rotational speed leads to a faster flow of oil-film, which in turn increases the collision frequency of fluid molecules and the subsequent interaction force decreases. Figure 5(d) plots the trajectory of bearing stiffness. Bearing stiffness, which represents the resistance to deformation, is crucial for evaluating the supporting characteristics of SGTB. With smaller spiral angle, a valuable stiffness of SGTB is exhibited across various rotational speeds. As the spiral angle increases, there is a significant decrease in bearing stiffness. It is evident that the spiral angle of SGTB has considerable impact on resisted deformation ability,

which should be carefully considered during the design process.

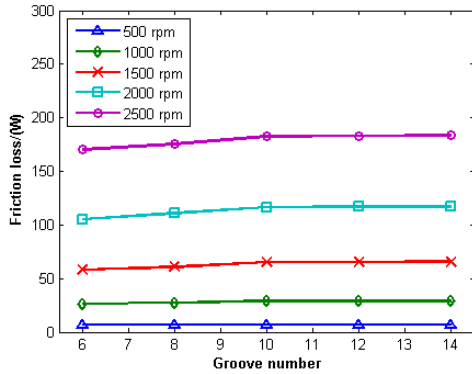
Figure 5(e) present the mitigative effect of oil-film under various working conditions, including spiral angle and rotational speed. It is observed that the damping coefficient decreases as the working speed increases. The rate of decline in damping coefficient almost follows the stable value at lower rotational speeds, which means the regularity is found in the variation trend. A turning point in the damping coefficient is noted at the condition ($\omega=1500$ rpm and $\alpha=40^\circ$), beyond which the damping coefficient changes smoothly. The damping coefficient is associated with bearing stiffness, and similar variation patterns occur under the same conditions. Meanwhile, Fig. 5(f) illustrates the cavitation volume fraction of SGTB with varying parameters, and the rotational speed varies from 500 rpm to 2500 rpm. In the condition ($\omega=500$ rpm and $\alpha=20^\circ$), the phase transition



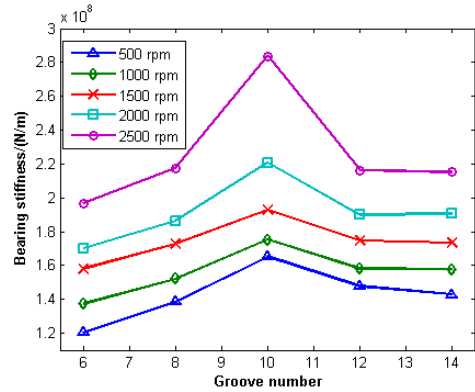
(a) Load carrying capacity



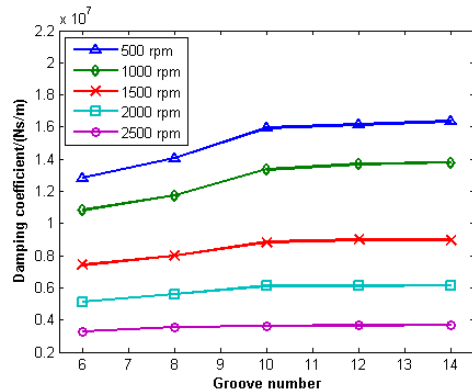
(b) Friction torque



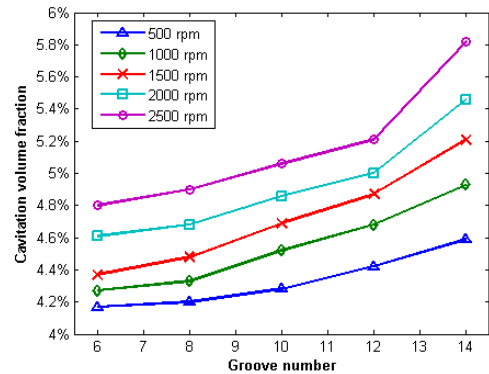
(c) Friction loss



(d) Bearing stiffness



(e) Damping coefficient



(f) Cavitation volume fraction

Fig. 6 Hydrodynamic behavior of SGTB with different groove numbers

characteristics of SGTB can be detected (4.22%) which means that the oil-film pressure is changed and continuity is damaged. However, this fraction changes to 4.91% under the condition ($\omega=2500$ rpm and $\alpha=20^\circ$). Thus, structural characteristics and operational parameters are major determinants of the cavitation volume fraction in SGTB.

4.2 Effects of Groove Number

Flow state and fluid velocity are decided by geometrical morphology of solid and the oil-film thickness is also changed by the variation of groove number. In case study, the groove numbers (8, 10, 12 and 14) and rotational speed (500 rpm, 1000 rpm, 1500 rpm, 2000 rpm and 2500 rpm) are chosen as the variables. Then, spiral angle and groove width ratio will be selected to 30° and 0.58, respectively. The coupled relationship between variables and lubrication feature of SGTB can

be revealed in this section.

The coupled influence of groove number and rotational speed on bearing capacity can be depicted in Fig. 6(a). The supporting force remains the stable value in the lower speed, but a growth trend is observable at higher speeds with varying groove numbers. As rotational speed increases, the load-carrying capacity of SGTB significantly improves. At lower fluid velocities, the oil film maintains a gradually varied flow, and the fluctuations in oil-film pressure are minimized. These results suggest that a well-matched design of groove number should be considered for optimal hydrodynamic lubrication in SGTB. Although changes in groove number and rotational speed can enhance the load-carrying capacity, they also increase the interaction forces among fluid molecules, leading to increased friction under the same conditions. Moreover, as shown in Fig. 6(b), this increase in friction torque can hinder the

flow of lubricant medium and enhance the energy loss. According to the variation characteristics, the internal force (fluid molecules) and external force (fluid-solid) rises sharply when the groove number is below 10. At a groove number of 6 and a rotational speed of 2500 rpm, the friction torque measures 0.5845 Nm. The friction phenomenon would become even more severe, as the growth of groove number. The friction torque slightly increases to 0.7109 Nm under the condition ($\omega=2500$ rpm and $n=10$). At a groove number of 14, the friction torque, compared to the thrust bearing with 10 grooves, shows only a 2.1% increase, indicating that rotational speed plays the main factor on friction torque.

Figure 6(c) presents the variation characteristics of friction loss across different conditions (structure and operating). Friction loss changes only slightly with an increase in groove number. However, higher rotational speeds result in significantly greater friction loss. At lower rotational speeds, the friction loss is considerably reduced; at 500 rpm, the maximum friction loss is approximately 7.071 W. Conversely, the minimum friction loss reaches to 170.2 W under the condition ($\omega=2500$ rpm and $n=6$). The noticeable increase in the proportion of friction loss underscores that the motion velocity of the fluid correlates with contact force and collision frequency among molecules. Figure 6(d) shows the anti-deformation ability of SGTB with respect to groove number is illustrated. Groove number is a critical factor affecting the bearing stiffness of SGTB. At a pivotal groove number of 10, there is a noticeable change in the resistance to deformation of oil-film. With a smaller groove number, the resistance ability of SGTB markedly promotes. However, the stiffness values drop abruptly when the groove number exceeds 10. This sudden decrease is due to changes in the structural features of the grooves, which alter the motion region of the lubrication oil. According to the law of momentum conservation, the pressure distribution within the oil-film varies with the fluid's motion velocity, resulting in inconsistent bearing stiffness values for SGTB.

Figure 6(e) depicts the damping coefficient of SGTB under various conditions. Observing the curve of the damping coefficient, it is evident that the damping coefficient at 500 rpm is higher than at other speeds. For instance, the damping coefficients of SGTB with groove numbers 6 and 14 have the obvious difference at the same rotational speed. Additionally, the intermolecular force can decide the deformation value of oil-film, and this phenomenon would be more pronounced as the groove number decreases. The relationship mapping cavitation volume fraction, groove number, and rotational speed is displayed in Fig. 6(f). The presence of cavitation impedes the flow of the lubrication medium, and the rupture of cavitation bubbles significantly alters the oil-film. Simulation results indicate that a decrease in groove number helps restrain cavitation formation, particularly when the groove number exceeds 12. Variations in rotational speed affect the pressure gradient in the low-pressure region. It is also noteworthy to consider the coupled effects of design parameters on the cavitation volume fraction in SGTB.

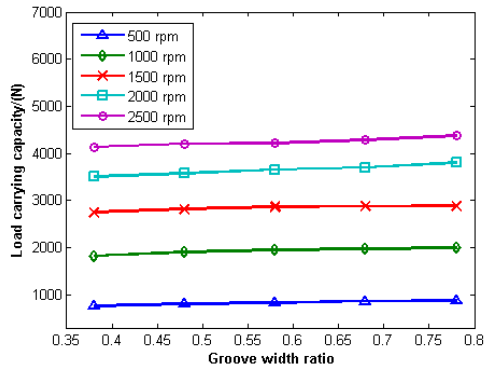
4.3 Effects of Groove Width Ratio

Groove width ratio is also one of design goal for SGTB, which decides the area proportion of groove in bearing. In simulation model, the spiral angle and groove number are selected constant values. The rotational speeds are chosen as variable (500 rpm, 1000 rpm, 1500 rpm, 2000rpm and 2500 rpm).

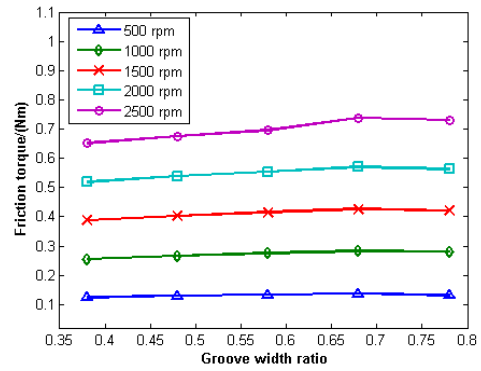
Figure 7(a) depicts the load-carrying capacity of SGTB is presented under various conditions. It is clearly observed that the bearing capacity increases gradually as the groove width ratio increases. This phenomenon can be attributed to the fact that changes in groove width ratio have a minimal impact on the flow pattern of lubricant medium, and the pressure values remain relatively stable. Similar lubrication characteristics are evident in the trajectory of friction torque, as shown in Fig. 7(b). Although the friction torque slightly increases at higher rotational speeds, the percentage of growth is minimal. However, the friction torque shows a decreasing trend under the condition ($w_r=0.78$). The values of bearing capacity and friction torque are closely related to intermolecular forces. Rotational speed is a relatively sensitive factor affecting these values. For instance, under the condition ($w_r=0.38$), the load-carrying capacities of SGTB at rotational speeds of 500 rpm and 2500 rpm are 758.99 N and 4138.31 N, respectively. Higher rotational speeds enhance the oil-film pressure and molecular collision force, and also alter the velocity gradient.

The friction loss is the crucial appraisal indicator for evaluating the lubricant performance of SGTB, which can represent the energy change and execution efficiency of oil-film. Figure 7(c) illustrates that the difference sensitivity of friction loss is given by rotational speed and groove width ratio. Specifically, the flow characteristics would keep a stable value under the condition (smaller groove width ratio), and the variation of oil-film thickness just occurs in local region. The higher flow velocity of lubricant medium can cover up the minor changes in the near wall flow layer. However, this value increases to 7.18 W when groove width ratio reaches 0.78. At a rotational speed of 2500 rpm, the friction losses for groove width ratios of 0.38 and 0.78 are 170.5 W and 191.2 W, respectively, indicating a notable increase. Figure 7(d) reveals the slight variation in the characteristics of oil-film resistance force, but there is a significant decrease in the values under conditions where $w_r \geq 0.48$. Nonetheless, the bearing stiffness of SGTB exhibits a downward trend as the groove width ratio increases. The results demonstrate that both friction loss and bearing stiffness are higher at increased rotational speeds, suggesting that the operational conditions can alter the intermolecular forces and flow characteristics.

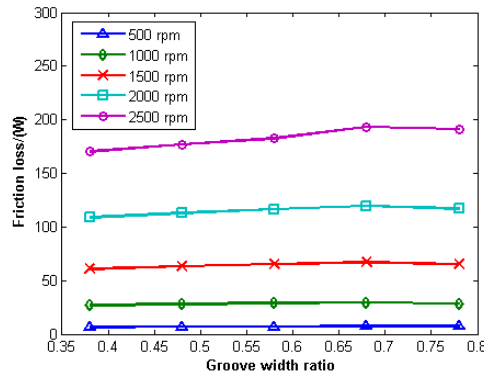
The response of damping coefficient under variation conditions is presented in Fig. 7(e). The results show a significant initial decrease in the damping coefficient. In the condition where $w_r=0.48$, the rate of decrease in the damping coefficient slows down. As rotational speed increases, the rate of decrease in the damping coefficient across different groove widths gradually lessens.



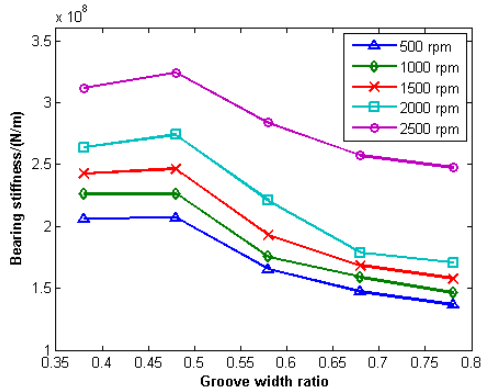
(a) Load carrying capacity



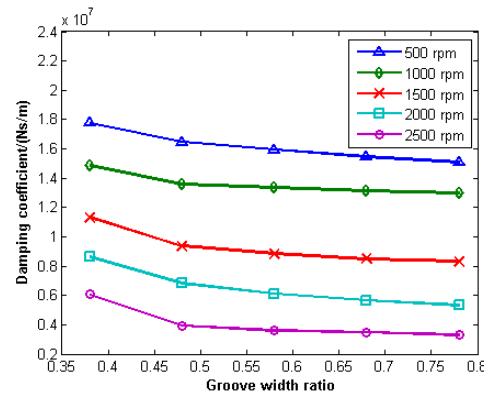
(b) Friction torque



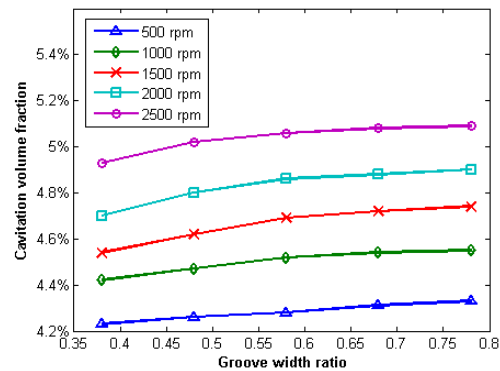
(c) Friction loss



(d) Bearing stiffness



(e) Damping coefficient



(f) Cavitation volume fraction

Fig. 7 Hydrodynamic behavior of SGTB with different groove width ratios.

Moreover, an increase in rotational speed leads to a decrease in the damping coefficient, which may elucidate the coupled influence of structure characteristics and operational parameters on lubrication features. According to the simulation results, as stated in Fig. 7(f), cavitation effects in SGTB are more likely to occur under conditions of higher rotational speeds and larger groove width ratios. An increase in rotational speed enhances the motion velocity of lubricant medium, and the flow pattern also changes with the variation in velocity gradient, potentially leading to cavitation effects. For example, at a lower rotation speed, the phase transition ratio is smaller, which means that the bubble is only found at the corner of groove. However, with the increase of rotation speed, the bubble would occur in the mainstream way. Additionally, the occurrence of cavitation effects leads to the accumulation of more bubbles. These bubbles move with the oil-film in inactive

regions, an outcome that is generally unintended by designers.

5. CONCLUSIONS

In this study, the hydrodynamic lubrication of SGTB with cavitation is thoroughly analyzed. Initially, a multi-phase flow model is integrated into the lubrication performance analysis model. The hydrodynamic responses of SGTB are obtained using the proposed model, and a comparative analysis between simulation and experimental results is conducted. The mapping relationship between parameters and lubrication properties of SGTB is discussed.

Furthermore, the study explores the hydrodynamic lubrication of SGTB under various conditions. The coupled effects of structural characteristics and motion parameters are shown to influence the flow

characteristics of the lubrication medium and the bearing's support performance in detail. The load-carrying capacity and damping coefficient are significantly affected by the spiral angle. Similarly, the values of cavitation volume fraction and friction torque for thrust bearings vary markedly with different groove numbers. Changes in groove width ratio directly impact friction loss. Additionally, bearing stiffness is found to be sensitive to the geometrical parameters of groove. The proposed method provides effective recommendations for the optimization and design of SGTB.

This work focuses on the lubrication ability of SGTB and the simulation model can be established one by one. In the future, the parametric modeling method can be introduced with the geometric features, which can improve the efficiency of simulation modelling.

ACKNOWLEDGEMENTS

This work is supported by the “National Natural Science Foundation of China (No. 52405140)”.

CONFLICT OF INTEREST

The author has no conflicts to disclose.

AUTHORS CONTRIBUTION

Liu Kailei: Writing - review & editing. **Chen Jiayuan:** Data-curation and analysis. **Zhu Haoran:** Investigation. **Zhang Lin:** Methodology and Software. **Wu Xuze:** Validation and Visualization. **Chen Yu:** Writing – original draft.

REFERENCES

- Bai, L. Q., & Bai, S. X. (2014). Frictional performance of a textured surface with elliptical dimples: geometric and distribution effects, *Tribology Transactions*, 57(6), 1122-1128. <https://doi.org/10.1080/10402004.2014.939317>
- Chetti, B. (2016). The effect of turbulence on the performance of a two-lobe journal bearing lubricated with a couple stress fluid. *Industrial Lubrication and Tribology*, 68(3), 336-340. <https://doi.org/10.1108/ILT-06-2015-0072>
- Eleshaky, M. E. (2009). CFD investigation of pressure depressions in aerostatic circular thrust bearings. *Tribology International*, 42, 1108-1117. <https://doi.org/10.1016/j.triboint.2009.03.011>
- Fesanghary, M., & Khonsari, M. M. (2013). On the optimum groove shapes for load-carrying capacity enhancement in parallel flat surface bearing: theory and experiment. *Tribology International*, 67, 254-262. <https://doi.org/10.1016/j.triboint.2013.08.001>
- Gao, S. Y., Cheng, K., & Chen, S. J. (2015). CFD based investigation on influence of orifice chamber shapes for the design of aerostatic thrust bearings ay ultra-high speed spindles. *Tribology International*, 92, 211-221. <https://doi.org/10.1016/j.triboint.2015.06.020>
- Gherca, A., Fatu, A., & Hajjam, M. (2016). Influence of surface texturing on the hydrodynamic performance of a thrust bearing operating in steady-state and transient lubrication regime. *Tribology International*, 102, 305-318. <https://doi.org/10.1016/j.triboint.2016.05.041>
- Gropper, D., Harvey, T. J., & Wang, L. (2018). A numerical model for design and optimization of surface textures for tilting pad thrust bearings. *Tribology International*, 119, 190-207. <https://doi.org/10.1016/j.triboint.2017.10.024>
- Hu, Y., & Meng, T. G. (2019). Theoretical and experimental study of transient behavior of spiral-groove thrust bearings during start-up. *Tribology Transactions*, 31(5), 2083-2091. <https://doi.org/10.1080/10402004.2019.1670887>
- Kim, M. S., Shim, J., & Kim, J. (2020). Multiphysics simulation and experiment of a thrust bearing in scroll compressors. *Tribology International*, 142: 105969. <https://doi.org/10.1016/j.triboint.2019.105969>
- Lin, X. H., Jiang, S. Y., & Zhang, C. B. (2018). Thermohydrodynamic analysis of high speed water-lubricated spiral groove thrust bearing considering effects of cavitation, inertia and turbulence. *Tribology International*, 119: 645-658. <https://doi.org/10.1016/j.triboint.2017.11.037>
- Lin, X. H., Wang, R. Q., & Jiang, S. Y. (2020). Study on dynamic characteristics for high speed water-lubricated spiral groove thrust bearing considering cavitating effect. *Tribology International*, 143, 106022. <https://doi.org/10.1016/j.triboint.2019.106022>
- Mao, Y., Zeng, L. C., & Lu, Y. (2016). Modeling and optimization of cavitation on a textured cylinder surface coupled with the wedge effect. *Tribology International*, 104, 212-224. <https://doi.org/10.1016/j.triboint.2016.09.002>
- Meng, F. M., & Yang, T. (2013). Preliminary study on mechanism of cavitation in lubricant of textured sliding bearing. *Proceedings of the Institution of Mechanical Engineers, Part J, Journal of Engineering Tribology*, 227(7), 695-708. <https://doi.org/10.1177/1350650112468560>
- Meng, F. M., Zhang, L., & Liu, Y. (2015). Effect of compound dimple on tribological performances of journal bearing. *Tribology International*, 91: 99-110. <https://doi.org/10.1016/j.triboint.2015.06.030>
- Meng, X. K., Bai, S. X., & Peng, X. D. (2014). Lubrication film flow control by oriented dimples for liquid lubricated mechanical seals. *Tribology International*, 77, 132-141. <https://doi.org/10.1016/j.triboint.2014.04.020>
- Ochiai, M., Sunami, Y., & Hashimoto, H. (2014). Study on angular displacement characteristics on

- topological optimum design problem of hydrodynamic thrust air bearing. *Proceedings of the Institution of Mechanical Engineers, Part J, Journal of Engineering Tribology*, 228(9), 997-1007. <https://doi.org/10.1177/1350650114534835>
- Pavel, N., Jozef, H., & Jaroslav, J. (2019). Effective thrust bearing model for simulations of transient rotor dynamics. *International Journal of Mechanical Sciences*, 157-158, 374-383. <https://doi.org/10.1016/j.ijmecsci.2019.04.057>
- Rao, T. V. V. L. N., Rani, A. M. A., & Mohamed, N. M. (2019). Analysis of magnetohydrodynamic partial slip laser bump texture slider and journal bearing. *Proceedings of the Institution of Mechanical Engineers, Part J, Journal of Engineering Tribology*, 233(12), 1921-1938. <https://doi.org/10.1177/1350650119852568>
- Xu, W. J., & Yang, J. G. (2016). Spiral-grooved gas face seal for steam turbine shroud tip leakage reduction: performance and feasibility analysis. *Tribology International*, 98, 242-252. <https://doi.org/10.1016/j.triboint.2016.02.035>
- Zhang, J. B., Zou, D. L., & Rao, Z. S. (2018). A numerical method for solution of the discharge coefficients in externally pressurized gas bearings with inherent orifice restrictors. *Tribology International*, 125, 156-168. <https://doi.org/10.1016/j.triboint.2018.03.009>
- Zhang, J. B., Zou, D. L., & Rao, Z. S. (2018). Numerical research of pressure depression in aerostatic thrust bearing with inherent orifice. *Tribology International*, 123, 385-396. <https://doi.org/10.1016/j.triboint.2018.03.009>
- Zhang, X. Q., Wang, X. L., & Liu, R. (2013). Influence of temperature on nonlinear dynamic characteristics of spiral-grooved gas-lubricated thrust bearing-rotor systems for microengine. *Tribology International*, 61, 138-143. <https://doi.org/10.1016/j.triboint.2012.12.013>
- Zhao, Y., Wei, C., & Yuan, S. (2016). Theoretical and experimental study of cavitation effects on the dynamic characteristic of spiral-groove rotary seals (SGRSs). *Tribology Letters*, 64(3), 1-18. <https://doi.org/10.1007/s11249-016-0784-6>
- Zouzoulas, V., & Papadopoulos, C. I. (2017). 3-D thermohydrodynamic analysis of textured, grooved, pocketed and hydrophobic pivoted-pad thrust bearings. *Tribology International*, 110, 426-440. <https://doi.org/10.1016/j.triboint.2016.10.001>